



Simple voltammetric approach for characterization of two-step surface electrode mechanism in protein-film voltammetry

Rubin Gulaboski¹ · Valentin Mirceski^{2,3}

Received: 13 March 2020 / Revised: 18 March 2020 / Accepted: 18 March 2020 / Published online: 16 April 2020
© Springer-Verlag GmbH Germany, part of Springer Nature 2020

Abstract

Many enzymes embedding multivalent metal ions or quinone moieties as redox-active centres undergo electrochemical transformation via two successive electron transfer steps. If electrochemical features of such redox enzymes are analyzed with “protein-film voltammetry”, one frequently meets a challenging reaction scenario where the two electron transfers take place at the same formal potential. Under such conditions, one observes voltammogram with a single oxidation-reduction pattern hiding voltammetric features of both redox reactions. By exploring some aspects of the two-step surface EECrev mechanism one can develop simple methodology under conditions of square-wave voltammetry to enable recognizing and characterizing each electron transfer step. The method relies on the voltammetric features of the second electron transfer, which is coupled to a follow-up chemical reaction. The response of the second electron transfer step shifts to more positive potentials by increasing the rate of the chemical reaction. The proposed methodology can be experimentally applied by modifying the concentration of an electrochemically inactive substrate, which affects the rate of the follow-up chemical reaction. The final voltammetric output is represented by two well-separated square-wave voltammetric peaks that can be further exploited for complete thermodynamic and kinetic analysis of the EECrev mechanism.

Keywords Square-wave voltammetry · Two-step electrode mechanism · Kinetics of electron transfer · Protein-film voltammetry

Introduction

Protein-film voltammetry is a valuable methodology introduced about two decades ago that enables an insight into important electrochemical and chemical features of many enzymes [1–5]. By adsorption of a given lipophilic enzyme on the surface of a working electrode one prepares an enzyme-modified electrode, which is suitable for exploration of protein

redox chemistry by means of a common three-electrode setup. Valuable data about mechanisms of action of many proteins, as well as important thermodynamic and kinetic parameters of the redox transformations of many enzymes, have been obtained in the last 20 years [1–5].

Many of the analyzed enzymes, in particular those featuring multivalent redox centres, exhibit rather complex electrochemical behaviour [1, 4, 5]. Such group can be exemplified with redox enzymes having quinone/hydroquinone moiety [6], or polyvalent cations of Mo, V, W or Mn [1, 3, 7–10] in the structure. Since many of these enzymes can undergo electrochemical transformation via successive exchange of electrons with the working electrode, their voltammetric patterns can be exceptionally complex [1–5]. As it is described in [11], their complex electrochemistry can be successfully resolved by square-wave voltammetry (SWV). In the theoretical models related to the two-step successive electrode mechanisms of [11–20], it has been recently reported on reliable procedures to characterize particular electrode enzymatic mechanism, in which coupled chemical steps occur. Moreover, relatively simple methodology has been elaborated

We dedicate this work on the occasion of the 65th birthday of our supervisor and great friend, professor Fritz Scholz.

✉ Rubin Gulaboski
rubin.gulaboski@ugd.edu.mk

¹ Faculty of Medical Sciences, Goce Delcev University, Stip, Macedonia

² Department of Chemistry, Faculty of Natural Sciences and Mathematics, Ss Cyril and Methodius University, Skopje, Macedonia

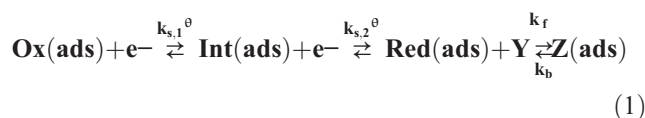
³ Department of Inorganic and Analytical Chemistry, University of Lodz, Tamka 12, Łódź, Poland

for determination of thermodynamic and kinetic parameters relevant to both electron transfers and the coupled chemical reactions [11, 14–20].

When voltammetric peaks related to both electrode reaction steps of a given redox enzyme are separated for at least [150 mV], it is easily achievable to determine all relevant kinetic and thermodynamic parameters of the two redox steps [11, 16–19]. However, if the two electron transfers take place at the same potential, the overall electrode mechanism is associated with a SW voltammogram featuring single oxidation-reduction voltammetric pattern. Under such conditions, it is quite difficult to recognize whether the existing peak is due to a single two-electron transfer step, or it is a consequence of two, successive one-electron electrode transformations. Hence, in the current work, we focus on developing an approach in SWV to recognize a two-step successive surface electrode mechanism, under conditions where both electron transfer steps occur at the same potential. The methodology presented could help researchers working in enzymatic electrochemistry to design proper voltammetric experiments for recognizing particular two-step surface electrode reaction. To the best of our knowledge, the methodology presented in this work has not been considered so far in the theory of square-wave voltammetry of two-step electrode mechanisms [11–20]. It is finally worth mentioning that the current study is also adequate to analyse the so-called “surface electrode mechanisms” [21–24], i.e. electrode reactions taking place exclusively from an adsorbed state.

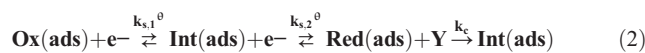
Details of theoretical models

Electrode mechanisms consisting of two successive electron transfers, coupled with a follow-up chemical reaction to the second electrode step, are analyzed under conditions of protein-film square-wave voltammetry. The first mechanism is the so-called “surface EECrev”, while the second one is “surface EEC’ catalytic” mechanism. In the abbreviation for the “surface EECrev mechanism”, the term “E” describes the electron transfer step, while “Crev” refers to a reversible chemical reaction. In the surface EEC’ mechanism, the symbol C’ stands for a regenerative chemical reaction. In both mechanisms, we consider an enzymatic electrode transformation with all species firmly immobilized on the surface of the working electrode. The electrode transformation of the initial enzymatic form Ox(ads) to the final redox form Red(ads) in both mechanisms occurs in two successive one-electron steps. In mechanism (1), we assume that the final enzymatic product (Red(ads)) undergoes follow-up reversible chemical reaction with an electrochemically inactive substrate “Y”. Schematic representation of such process (mechanism (1)) is as follows:



Only enzymatic species Ox(ads) are present on the electrode surface at the beginning of the experiment. In a first approximation, it has been assumed that all immobilized species are uniformly adsorbed (“ads”) without any lateral interactions. With Int(ads), we assign electroactive enzymatic species formed as an intermediate in the first electrode reduction step. With Red(ads), we assign the final redox-active enzymatic species, generated electrochemically during the second electrode transfer step from Int(ads). With “Y”, we define species present in the electrochemical cell that show no electrochemical activity in the potential region used for the voltammetric experiment. Y is supposed to react in a selective and chemically reversible fashion with Red(ads) species, converting them to the final electrochemically inactive product Z(ads) (reaction Eq. 1).

The second electrode mechanism considered is the so-called “surface catalytic EEC’ mechanism”, also known as a “surface regenerative EEC’ mechanism”, which can be described with reaction Eq. (2):



The major difference between mechanisms (1) and (2) is seen in the nature of the chemical reaction. Indeed, in mechanism (2), it is assumed that the electrochemically inactive reactant “Y” irreversibly reacts with Red(ads), in a way to regenerate the intermediate Int(ads). In both mechanisms, we assume that the “Y” substrate is present in a large excess in the electrochemical cell. Therefore, we assume that the concentration of “Y” is constant on the electrode surface in the course of the voltammetric experiment. Consequently, the chemical steps in both mechanisms are assumed to be of a pseudo-first order in terms of chemical kinetics.

Both mechanisms are solved under the following boundary conditions:

$$t = 0; \Gamma(\text{Ox}) = \Gamma^*(\text{Ox}); \Gamma(\text{Int}) + \Gamma(\text{Red}) + \Gamma(\text{Z}) = 0$$

For $t > 0$, the following conditions apply:

$$t > 0; \Gamma(\text{Ox}) + \Gamma(\text{Int}) + \Gamma(\text{Red}) + \Gamma(\text{Z}) = \Gamma^*(\text{Ox}) \quad (\text{for mechanism 1})$$

$$t > 0; \Gamma(\text{Ox}) + \Gamma(\text{Int}) + \Gamma(\text{Red}) = \Gamma^*(\text{Ox}) \quad (\text{for mechanism 2})$$

$$d\Gamma(\text{Ox})/dt = -I_1/(FS) \quad (\text{for mechanisms 1 and 2})$$

$$d\Gamma(\text{Int})/dt = I_1/(FS) - I_2/(FS) \quad (\text{for mechanisms 1 and 2})$$

$$d\Gamma(\text{Red})/dt = I_2/(FS) - k_f\Gamma(\text{Red}) + k_b\Gamma(\text{Z}) \quad (\text{for mechanism 1})$$

$$d\Gamma(\text{Int})/dt = I_1/(FS) - I_2/(FS) + k_c\Gamma(\text{Red}) \quad (\text{for mechanism 2})$$

$$d\Gamma(\text{Red})/dt = I_2/(FS) - k_c\Gamma(\text{Red}) \quad (\text{for mechanism 2})$$

In both models, we assume that Butler-Volmer formalism applies for the interdependence of the electric potential (E), the current (I), the electrode reaction kinetic parameters (i.e. the standard rate constant k_s^\ominus and electron transfer coefficient α) and the surface concentration Γ . The analytical solutions of electrode mechanisms (1) and (2) are given in [11, 17], respectively. In [17], a detailed MATHCAD file containing all recurrent formulas for calculating SW voltammograms of the surface EECrev mechanism is provided.

In both mechanisms, we consider reduction currents as positive, and negative sign is ascribed to oxidation currents. All theoretical voltammograms are presented versus the formal potential of the first electrode process (assigned as a “peak I”).

Critical parameters controlling voltammetric behaviour

Dimensionless current Ψ of calculated voltammograms for both mechanisms is defined as a sum of partial currents related to the first (Ψ_1) and the second (Ψ_{II}) electrode step: $\Psi = \Psi_1 + \Psi_{II}$. Each dimensionless current, related to the corresponding electron transfer step, is normalized as follows: $\Psi_1 = I_1/[FSfT(\text{Ox})^*]$ and $\Psi_{II} = I_2/[FSfT(\text{Ox})^*]$. Here, S is the active surface area of working electrode and f is the frequency of SW pulses defined as $f = 1/(2t_p)$, where t_p is the duration time of a single potential pulse in SWV. $\Gamma(\text{Ox})^*$ stands for the total surface concentration, which corresponds to the surface concentration of the initially adsorbed Ox(ads) species. The potential driving force of each electrode reactions defined in a form of a dimensionless potentials is: $\Phi_1 = F(E - E_1^\ominus)/RT$ and $\Phi_2 = F(E - E_2^\ominus)/RT$, where E_1^\ominus and E_2^\ominus are the standard redox potential of the first and second electrode steps, respectively. T is symbol of the thermodynamic temperature (it was set to 298 K in all simulations), R is universal gas constant and F is the Faraday constant.

Features of simulated SW voltammetric patterns depend on several dimensionless parameters as follows. (a) The dimensionless electrode kinetic parameters related to each electron transfers: $KI = k_{s,1}^\ominus/f$ and $KII = k_{s,2}^\ominus/f$. Both KI and KII reflect the influence of the electrode kinetics represented by the standard rate constants ($k_{s,1}^\ominus$ and $k_{s,2}^\ominus$) relative to the critical time window of the experiment (i.e. SW frequency, f).

(b) For the surface EECrev mechanism, dimensionless chemical parameter $K_{\text{chemical}} = \varepsilon/f$ affects the features of SW voltammograms. In the last equation, ε is the cumulative rate constant $\varepsilon = (k_f + k_b)$, where k_f and k_b are the rate constants of the forward and backward chemical reaction, respectively.

Hence, the dimensionless parameter K_{chemical} reflects the effect of the chemical kinetics, relative to the time window of the SW experiment. In addition, mechanism (1) is affected by the equilibrium constant defined as $K_{\text{eq}} = k_f/k_b$.

(c) For the surface catalytic EEC' mechanism, the dimensionless chemical kinetic parameter is defined as $K_{\text{catalytic}} = k_c/f$. In last equation, k_c is the rate constant of the regenerative (catalytic) chemical reaction. At this stage, it is worth to emphasize that both chemical parameters related to the chemical steps (ε and k_c) are of pseudo-first order. Both, ε and k_c , depend on the concentration of substrate “Y” as follows: $\varepsilon = [k_f^\ominus c(Y) + k_b]$ for the mechanism (1) and $k_c = k_c^\ominus c(Y)$ for the mechanism (2). In the last equations, k_f^\ominus and k_c^\ominus are real, second-order chemical rate constants, while $c(Y)$ is the molar concentration of the substrate Y, which remains constant in the course of the experiment.

The parameters of applied potential in all calculations were set to: SW frequency $f = 10$ Hz, SW amplitude $E_{\text{sw}} = 50$ mV, and potential step $dE = 4$ mV. In addition, electron transfer coefficient to both electron transfer steps and both mechanisms was set to $\alpha = 0.5$. The net SWV current at all voltammograms is represented by black colour, while blue colour is associated to the forward (reduction) currents. Red colour is associated to the backward currents of all calculated voltammograms.

Results and discussions

In previous works, we have presented comprehensive theoretical studies of the surface EE, ECE, EECirr, EECrev and EEC' mechanisms [11–20] under conditions of SWV. In [11, 17, 18], a set of relevant theoretical voltammetric features of the surface EECrev, EEC' and EECirr systems have been elaborated, respectively. A scenario for appearance of two SW peaks, separated for at least 150 mV (in absolute value), has been comprehensively analyzed for the surface EECirr, EECrev and EEC' mechanisms [11]. In order to understand voltammetric characteristics of the present EECrev mechanism when the formal potentials of the two-electron transfer steps are identical, we briefly recall a small segment of this mechanism under conditions when the two electrode reactions are separated in their formal redox potentials.

SW voltammograms calculated for potential difference of -300 mV between the second and the first electron transfer step are shown in Fig. 1. The figure depicts the effect of the dimensionless chemical rate parameter K_{chemical} calculated for $K_{\text{eq}} = 1$, $KI = 1.5$ and $KII = 1.78$. Since the rate of the chemical step affects directly the second electron transfer, one witnesses remarkable changes of peak II (positioned at more negative potentials) caused by the increasing of K_{chemical} . As the magnitude of K_{chemical} increases from 0.001 to 0.1, the intensity of all current components of the second process

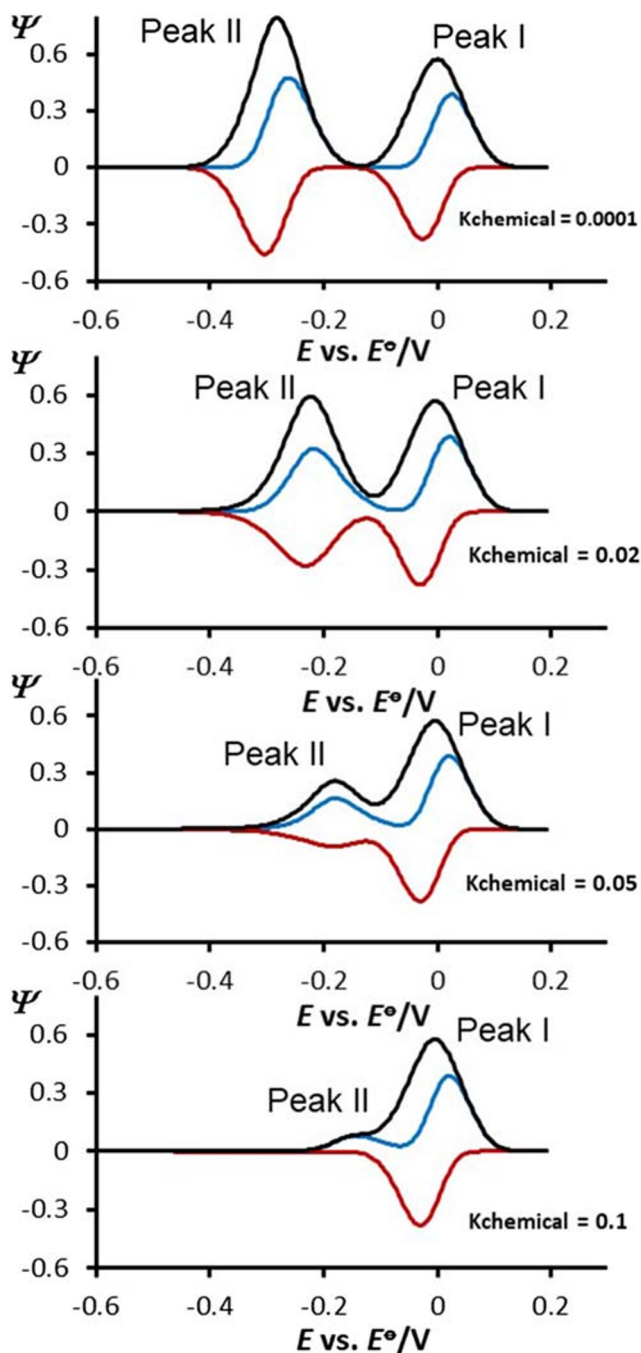


Fig. 1 Surface EECrev mechanism: square-wave voltammograms simulated for a potential separation of -300 mV between the second and the first electron transfer step. Voltammetric patterns reflect the effect of the chemical rate parameter K_{chemical} . The values of K_{chemical} are given in the charts. In the simulations, the value of the kinetic of electron transfer of the first electron transfer step was $K_{\text{I}} = 1.50$, while $K_{\text{II}} = 1.78$. The value of the equilibrium constant of the chemical reaction was set to $K_{\text{eq}} = 1$. Other simulation parameters were SW frequency $f = 10$ Hz, SW amplitude $E_{\text{sw}} = 50$ mV, potential step $dE = 4$ mV and temperature $T = 298$ K. In all simulations, the electron transfer coefficients of the first and second electrode reaction were set to the same value of $\alpha = 0.5$. The stoichiometric number of electrons exchanged was $n_1 = n_2 = 1$

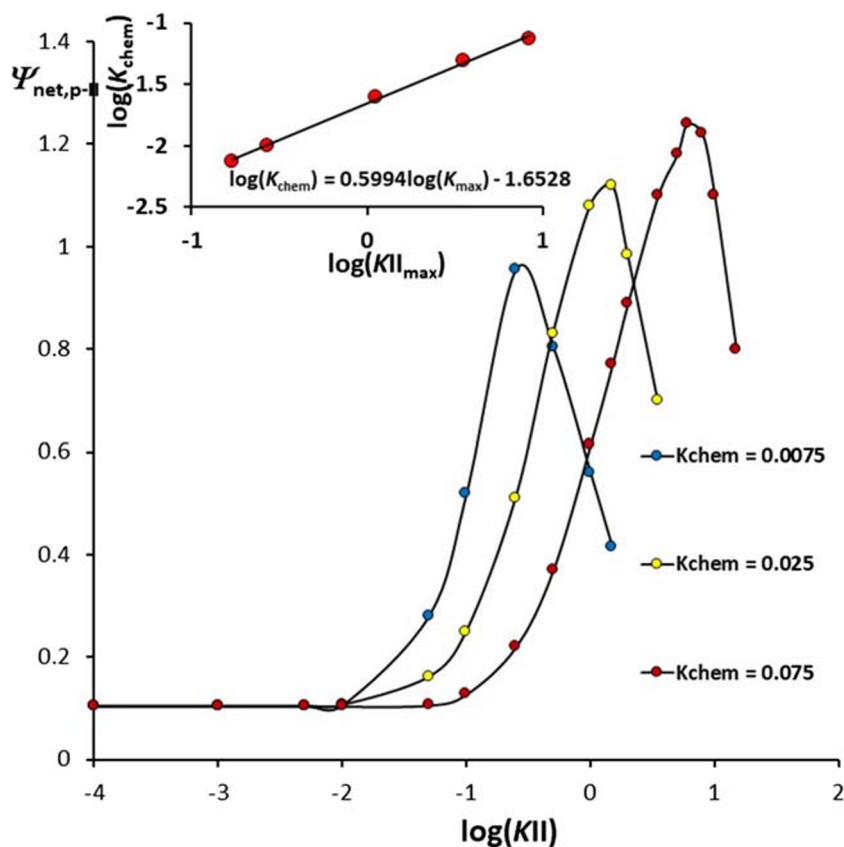
significantly diminishes. At the same time, the net peak potential of the second peak shifts for 59 mV/ n in a positive direction by a tenfold increase of K_{chemical} .

For $Keq \leq 10$, one observes very specific phenomenon; indeed, the dependence of the net peak current $\Psi_{\text{netp,II}}$ on the electrode kinetic parameter K_{II} features well-developed maximum, the position of which is a function of K_{chemical} (Fig. 2). As elaborated in [21, 22], this specific dependence known as a “quasireversible maximum” appears in all surface mechanisms. The quasireversible maximum of the surface EECrev mechanism is a consequence of the chronoamperometric properties of the system and the current sampling procedure applied in SWV. Important part of this behaviour is also ascribed to variation of the surface concentration of Red(ads) species with time in the so-called “dead time” of SW potential pulses [24], i.e. in the course of the pulse when the current is not sampled. In [11, 19, 20], a method has been proposed for estimation of the chemical parameter K_{chemical} by means of the linear function presented in Fig. 2, which represents the functional relationship of the maximum position versus the rate of the chemical reaction.

It is useful to recall that the rate of the follow-up chemical reaction causes even more complex effect to the voltammetric patterns of the surface EECrev mechanism when the electron transfer step is very fast. As elaborated in [21–24], a representative feature of all “fast” surface electrode mechanisms is the “splitting of the net SW peak” (see Fig. 3a). Under such conditions, when peak II and peak I are separated for at least -200 mV, an increase of the chemical reaction rate (i.e. $K_{\text{chemical}} > 0.001$) produces simultaneous increase of all current components of the peak II (Fig. 3b–d), contrary to the reasonable expectation the response to diminish. For $K_{\text{chemical}} > 0.01$, the net peak splitting vanishes (Fig. 3c), while the magnitude of both forward (reductive) and backward (oxidative) SW components increases for about 200 times (compare Fig. 3d with a). Eventually, for $K_{\text{chemical}} > 0.06$, all peak currents of the second process start diminishing, while peak II shifts to more positive potentials, as expected for an EECrev mechanism (Fig. 3e, f).

The origin of such specific and peculiar voltammetric behaviour is elaborated in more details in [19, 20, 24]. Briefly, fast electron transfer reaction coupled to chemical reactions having moderate-to-fast kinetics leads to formation of a significant amount of Red(ads) species at the beginning of a potential pulse (i.e. in the non-current measuring time segments) [24]. In the course of the pulse, the redox species approaches rapidly to redox equilibrium when the electrode reaction is fast. Thus, small current remains to be sampled at the end of the potential pulse. However, in the presence of a follow-up chemical reaction, the redox equilibrium cannot be established, causing the redox transformations to proceed significantly even at the end of the potential pulse when the current is being

Fig. 2 Surface EECrev mechanism: a series of quasireversible maxima calculated for $K_{eq} = 10$ for different rates of the chemical reaction. The calculated patterns correspond to the second SW voltammetric peak (peak II) positioned at more negative potentials. The inset shows the relationship between $\log(K_{\text{chemical}})$ and the logarithm of the electrode kinetic parameter $\log(K_{II_{\text{max}}})$ associated to the position of the quasireversible maximum. All other simulation parameters were the same as for Fig. 1



sampled. Consequently, both forward and backward SW components significantly increase by increasing the rate of the follow-up chemical reaction, while the splitting of the net peak vanishes [19, 20, 24]. As reported in [11, 19, 20], these voltammetric features can be exploited for evaluation of the kinetic and thermodynamic parameters of the second electrochemical step and the follow-up chemical reaction of the overall EECrev mechanism (cf. Figs. 1, 2 and 3).

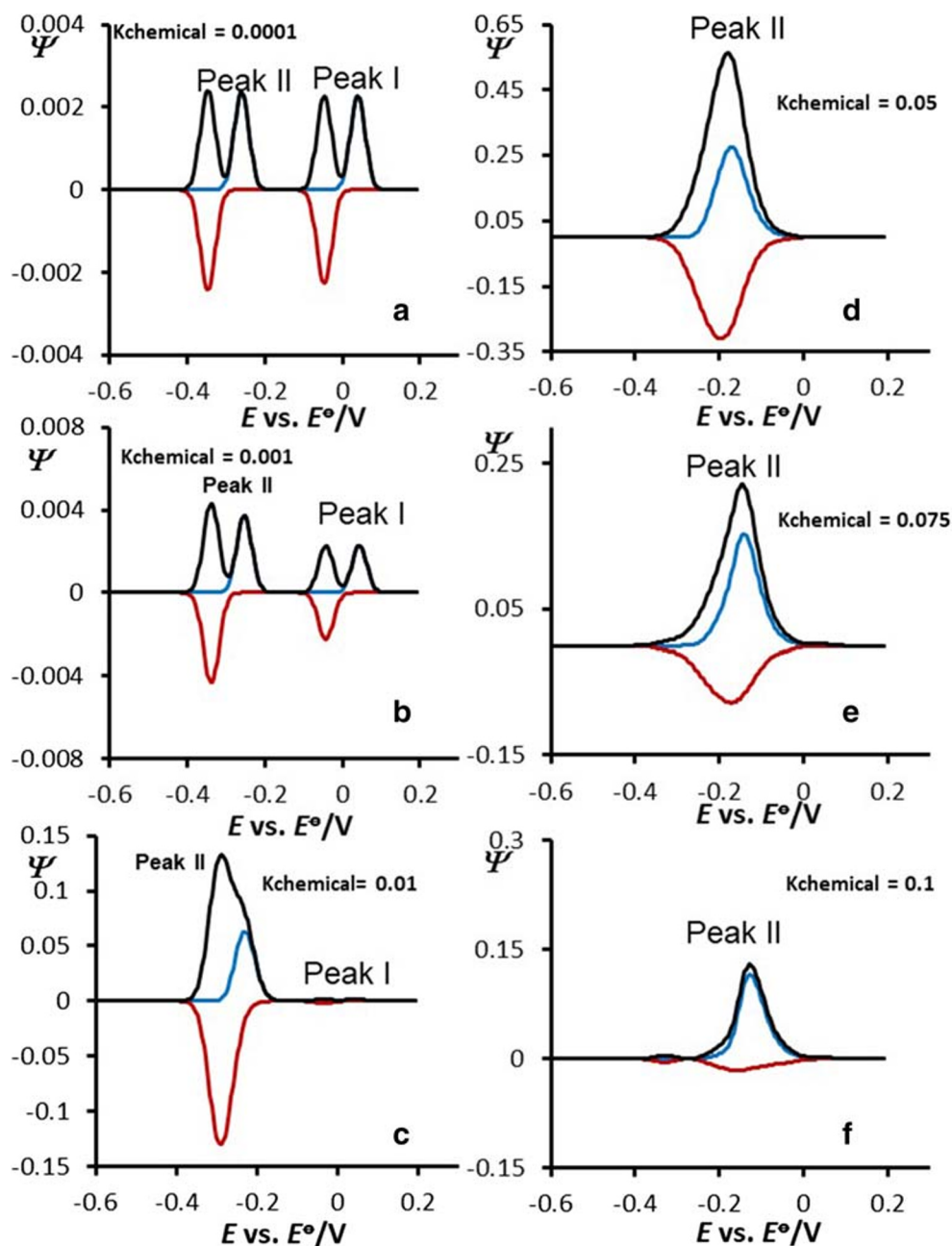
As briefly mentioned in the “Introduction” section, the most challenging situation for all two-step successive mechanisms is to characterize the two-electron transfer steps when they occur at the same potential. Under such circumstances, one observes SW voltammograms consisting of a single oxidation-reduction pattern, which “hides” features of both electron transfer steps (Fig. 4a). In such scenario, the major goal is to reveal whether the single voltammetric peak is due to a single, simultaneous two-electron transfer process, or it is a consequence of two successive one-electron transfer steps. Every misinterpretation of the “diagnosed” mechanism might lead to erroneous estimation of kinetic and thermodynamic parameters.

The first goal in such scenario is to find simple, qualitative criterion for recognizing the EECrev mechanism when the two-electron transfer steps are characterized with the same formal potential. The effect of the dimensionless chemical

parameter K_{chemical} to the voltammetric patterns is shown in Fig. 4. SW voltammograms are simulated for $K_{eq} = 0.1$, and electrode kinetic parameters $KI = 1.26$ and $KII = 2.82$. Following the discussions of the data presented in Figs. 1 and 3, and bearing in mind the features of the simple surface EC mechanism as a function K_{chemical} [11, 19, 20], one expects separation of both overlapped electron transfer steps to occur by increasing the rate of the follow-up chemical reaction. It is plausible to expect the kinetics of the chemical reaction to affect mainly voltammetric features of the second electron transfer (peak II). As presented in Figs. 1 and 3, an increase of the chemical reaction rate (expressed via K_{chemical}) shifts the second electron transfer process towards more positive potentials. Such scenario in Fig. 4 occurs for $K_{\text{chemical}} > 0.02$ (Fig. 4b). For $K_{\text{chemical}} > 0.05$ (Fig. 4d), one observes two well-separated processes: one at potential of 0.0 V (peak I), ascribed to the first electron transfer, and the second peak at about +0.15 V (peak II), associated to the second electron transfer step. Once the two processes are separated for at least 150 mV (Fig. 4d, e), one can apply the methodology for estimation of the kinetic parameters as elaborated in [11, 19–24].

Another interesting scenario is met in situation when both electron transfer steps of a surface EECrev mechanism are very fast, while taking place at the same formal potential. Under such conditions, one observes a single, split net SW peak (Fig. 5a). Again, via altering the value of K_{chemical} , one

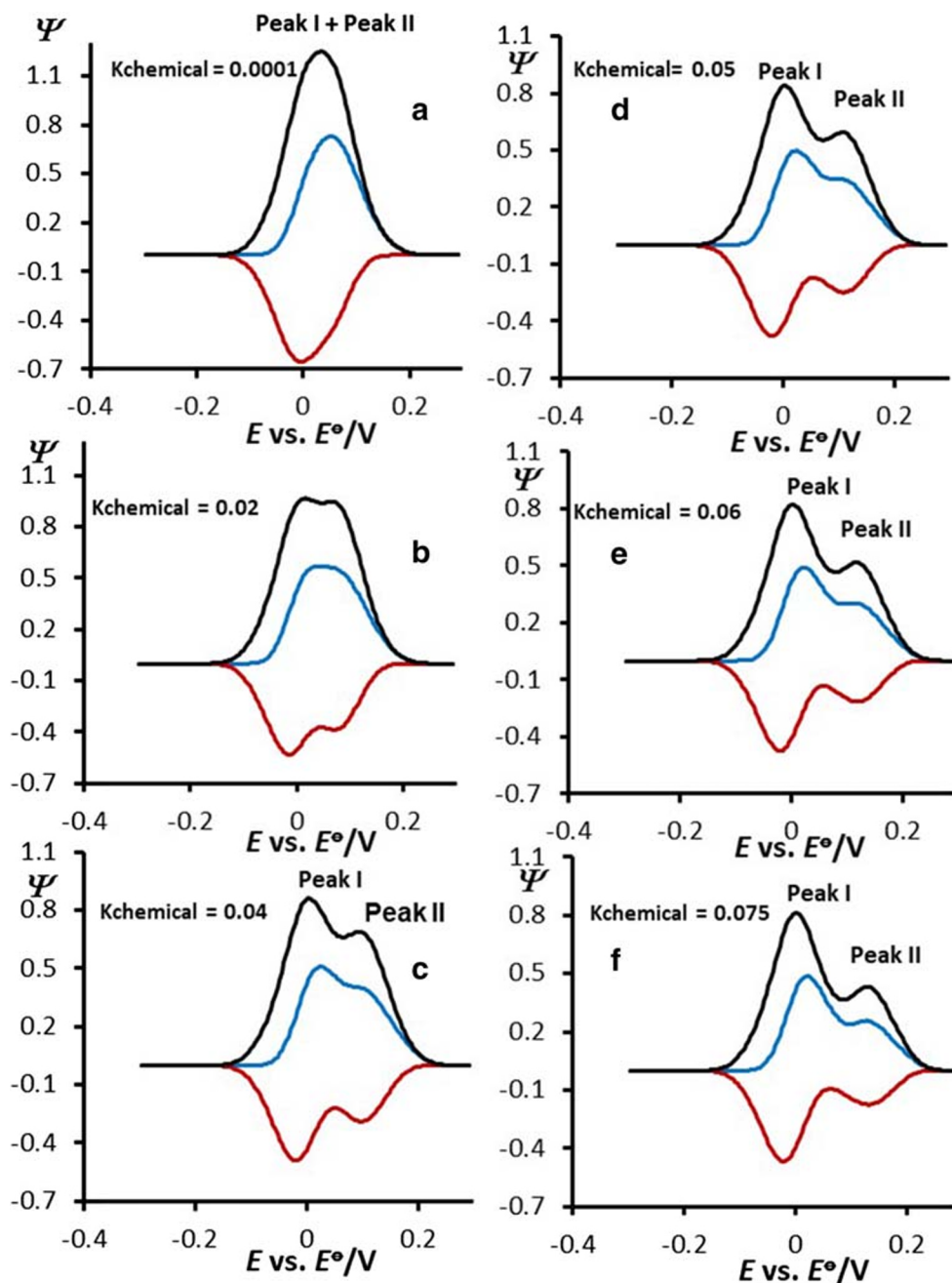
Fig. 3 Surface EEC_{rev} mechanism: square-wave voltammograms calculated for a potential difference of -300 mV between the second and the first electron transfer step. The voltammetric patterns show the effect of the chemical rate parameter K_{chemical} in the region of fast electron transfers of both steps ($K_{\text{I}} = 10$ and $K_{\text{II}} = 10$). The values of K_{chemical} are given in the charts. Value of the equilibrium constant of chemical reaction was set to $K_{\text{eq}} = 1000$. Other simulation parameters were the same as for Fig. 1



can achieve well separation between the two electron transfers, as represented in Fig. 5b–f. By increasing the magnitude of K_{chemical} , one can get a voltammetric pattern consisting of a “split SW net peak” that is related to the first electron transfer step (peak I), and a single net peak displaced to more positive potentials, which is associated to the second electron transfer that is coupled with the chemical reaction (peak II) (see Fig. 5e, f). From the voltammetric patterns (cf. Fig. 5e, f), one can estimate the values of K_{I} , K_{II} , K_{chemical} and K_{eq} . For the determination of K_{I} (peak I), one can use the method of “split net peak” [21, 23], while for determination of K_{II} , K_{chemical} and K_{eq} , one can utilize the methodology elaborated in [19–21, 24].

From the voltammetric profiles presented in Figs. 4 and 5, we recognize that the kinetics of the follow-up chemical reaction coupled to the second electron transfer might lead to a successful separation of two consecutive electron transfer steps, when these occur at the same potential. Theoretically speaking, one expects differentiation of the two-electron transfer steps to be possible for the EEC' catalytic mechanism as well. As shown in Fig. 6, an increase of the catalytic rate parameter $K_{\text{catalytic}}$ leads to the displacement of the second SWV peak to more negative potentials (see Fig. 6b–d), which is in agreement with previous data [11, 17, 25]. However, referring to voltammograms (Fig. 6b–d), it can be seen that the rate of the regenerative chemical reaction starts affecting the

Fig. 4 Surface EEC_{rev} mechanism: effect of the chemical rate parameter K_{chemical} to the voltammetric patterns, calculated when both electron transfers take place at the same potential. Voltammograms are simulated in the region of moderate rates of the electron transfer of both steps, i.e. $K_{\text{I}} = 1.26$ and $K_{\text{II}} = 2.82$. The values of K_{chemical} are given in the charts. Value of the equilibrium constant of chemical reaction was set to $K_{\text{eq}} = 0.1$. Other simulation parameters were the same as for Fig. 1



ascending branch of net peak at rather positive potentials. Consequently, the obtained catalytic current overlaps completely the response of the first electron transfer, which becomes completely invisible at higher rates of the regenerative reaction.

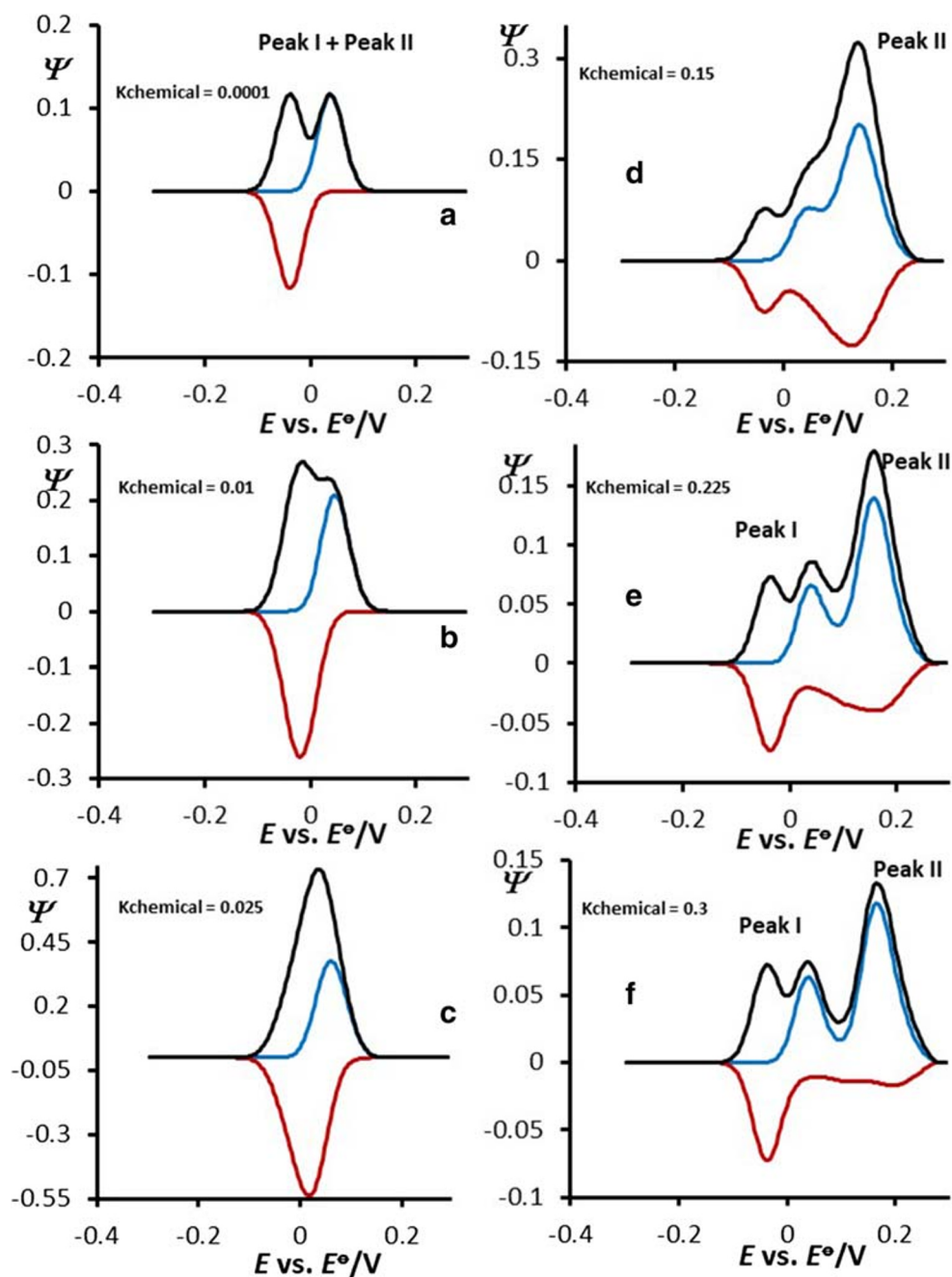
Voltammograms a'–d' in Fig. 6 are assigned to the first electron transfer step (peak I), being extracted out of the overall voltammograms Fig. 6a–d. The arrows show the position where peak I should appear in the overall voltammetric response. Because peak I is associated with peak II, we observe that peak I gets also slightly affected by $K_{\text{catalytic}}$. Its position shifts for 50 mV in a negative direction by increasing of $K_{\text{catalytic}}$ from 0.0001 to 0.04, while its height gets unaffected

at $K_{\text{catalytic}} > 0.04$. Unfortunately, the intensive catalytic current does not allow exploring the features of the separate electron transfer steps of the EEC' mechanism. This means that only via the features of the surface EEC_{rev} mechanism, as elaborated in Figs. 4 and 5, one can achieve efficient separation and characterization of the two-electron transfer steps.

Conclusions

Lipophilic enzymes containing multivalent ions or quinone moieties as redox-active centres are ubiquitous, while playing

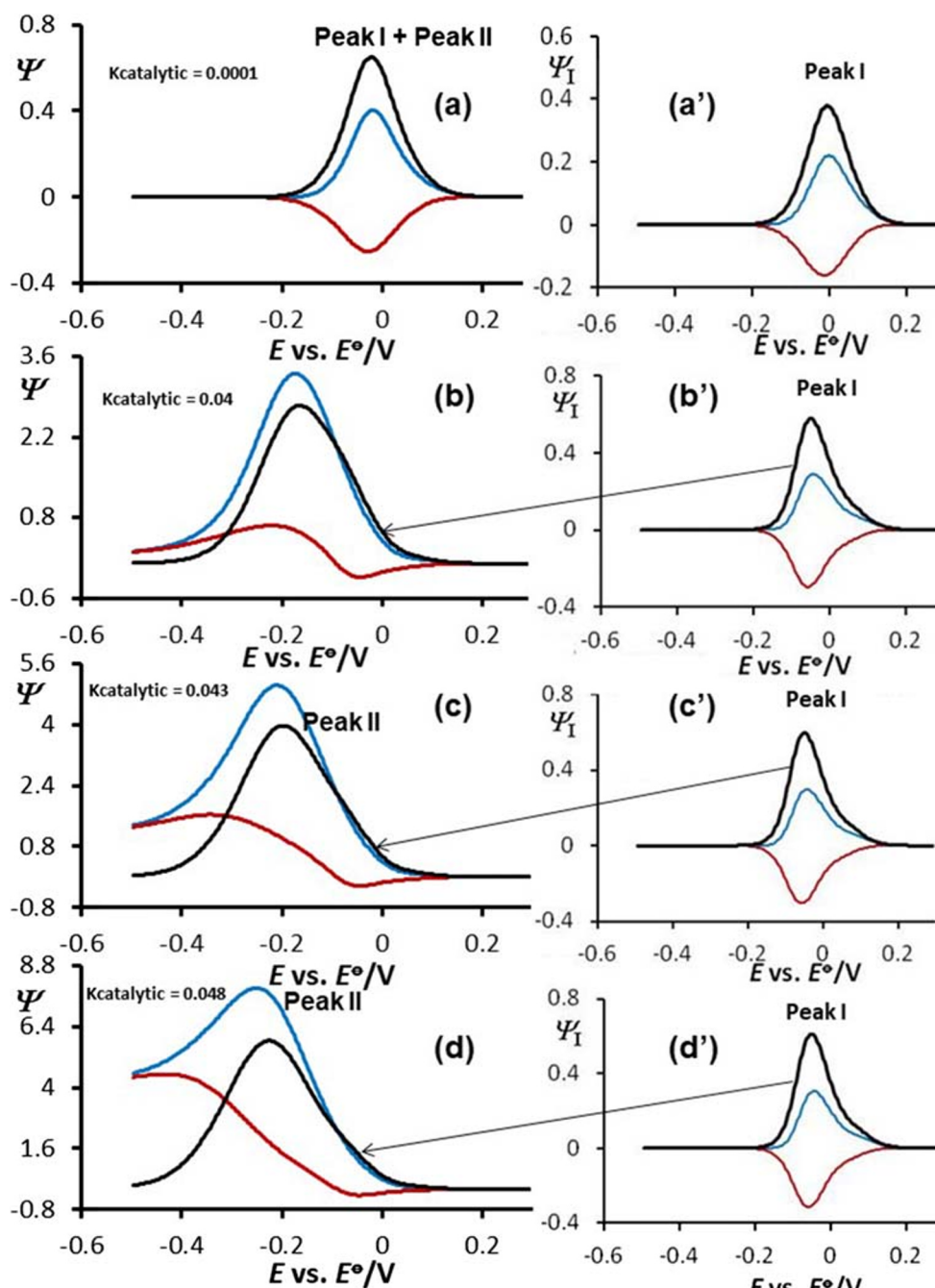
Fig. 5 Surface EECrev mechanism: effect of the chemical rate parameter K_{chemical} . All voltammetric patterns are calculated when both electron transfers take place as the same potential, in the region of fast rate of the electron transfer of both steps, i.e. $KI = 5$ and $KII = 5$. The values of K_{chemical} are given in the charts. Value of the equilibrium constant of chemical reaction was set to $K_{\text{eq}} = 100$. Other simulation parameters were the same as for Fig. 1



a crucial role in many cellular reactions. In the living systems, these enzymes can be turned into redox inactive state via follow-up chemical reaction [26]. The inactivation of many enzymes can provide important data about chemistry of the enzyme's active sites and on the catalytic potential. The electrochemical transformation of such enzymes commonly follows a pathway of successive electron transfers in two steps. If both electron transfer steps in such systems occur at the same potential, the electrochemistry of this class of enzymes will be portrayed in a single oxidation-reduction pattern when analyzed in “protein-film voltammetry”. The single square-wave voltammogram, obtained under defined circumstances,

will “hide” in its shape the features of both electron transfer steps. If this happens, a challenging task is to recognize the nature of electrode mechanism encountered in the analyzed system. In this work, we focused on developing efficient method to evaluate the two-step electrode mechanism, when both steps take place at same potential, by exploring the features of surface EECrev mechanism in SWV. As elaborated in this work, increased rate of the follow-up chemical reaction, expressed via K_{chemical} , displaces the second electron transfer process of a surface EECrev mechanism towards more positive potentials. Consequently, one can explore this feature to separate the two EE steps, if both happen at the same potential.

Fig. 6 Surface EEC' catalytic mechanism: **a–d** Effect of the catalytic rate parameter $K_{\text{catalytic}}$. All voltammograms are calculated when both electron transfers take place at the same potential, in the region of slow rate of the electron transfer of both steps, i.e. $KI = 0.2$ and $KII = 0.2$. The values of $K_{\text{catalytic}}$ are given in the charts. The panels (a'–d') correspond to the currents of peak I, extracted from the net SW voltammograms **a–d**. Other simulation parameters were the same as for Fig. 1



If we recall that the dimensionless chemical rate parameter K_{chemical} in surface EECrev mechanism is defined as $K_{\text{chemical}} = [k_f c(Y) + k_b]/f$, we recognize that modification of magnitude of K_{chemical} can be achieved in two ways: (a) via altering the SW frequency f and (b) via altering the concentration of substrate Y . Because the SW frequency affects simultaneously the rates of electron transfer of both steps (via KI and KII) and the magnitude of dimensionless chemical parameter K_{chemical} , altering the SW frequency will produce complex voltammograms. Therefore, in order to obtain voltammograms that will enable separation of the two

EE processes happening at same potential, modification of the rate of chemical reaction should be achieved via modification of the concentration of $c(Y)$. It is important to mention that these experiments in SWV should be performed at a constant frequency. Once we get voltammograms with separated peaks, as those presented in Figs. 4e and 5e, for example, then we can apply suitable methodologies for thermodynamic and kinetic evaluations related to both EE steps. For the determination of the electron transfer coefficient α of both steps, one should explore the methodology elaborated in [27].

Acknowledgements VM acknowledges with gratitude the financial support through the NATO SPS G5550 project (Gas sensors for preventing terrorist attacks), while RG thanks the “Goce Delcev” University in Stip, Macedonia for the support.

References

1. Armstrong FA (2015) Electrifying metalloenzymes in metalloproteins: theory, calculations and experiments (Cho AE, Goddar III WA, eds), CRC Press. Taylor&Francis Group, London
2. Leger C, Elliott SJ, Hoke KR, Jeuken LJC, Jones AK, Armstrong FA (2003) Enzyme electrokinetics: using protein-film voltammetry to investigate redox enzymes and their mechanism. *Biochem* 42: 8653–8662
3. Armstrong FA, Heering HA, Hirst J (1997) Reactions of complex metalloproteins studied by protein-film voltammetry. *Chem Soc Rev* 26:169
4. Armstrong FA (2002) Voltammetry of proteins. in: *Encyclopaedia of electrochemistry* (Bard AJ, Stratmann M, Wilson GS, eds), Wiley VCH, Weinheim
5. Jenner LP, Butt JN (2018) Electrochemistry of surface-confined enzymes: inspiration, insight and opportunity for sustainable biotechnology. *Curr Opin Electrochem* 8:81–88
6. Sies H, Parker L (2004) Quinones and quinone enzymes, in: *methods in enzymology*. Academic Press, London
7. Kobayashi M, Shimizu S (1999) Cobalt proteins. *Eur J Biochem* 261(1):1–9
8. Hille R (2002) Molybdenum and tungsten in biology. *Trends Biochem Sci* 27(7):360–367
9. Crans DC, Smee JJ, Galdamauskas E, Yang L (2004) The chemistry and biochemistry of vanadium and the biological activities exerted by vanadium compounds. *Chem Rev* 104(2):849–902
10. Ermler U, Grabarse W, Shima S, Goubeaud M, Thauer RK (1998) Active sites of transition-metal enzymes with focus on a nickel. *Curr Opin Struct Biol* 8(6):749–758
11. Janeva M, Kokoskarova P, Maksimova V, Gulaboski R (2019) Square-wave voltammetry of two-step surface redox mechanisms coupled with chemical reactions—a theoretical overview. *Electroanal* 31:2488–2506
12. Gulaboski R, Mirceski V, Bogeski I, Hoth M (2012) Protein-film voltammetry-electrochemical enzymatic spectroscopy: a review on recent progress. *J Solid State Electrochem* 16:2315–2328
13. Gulaboski R, Kokoskarova P, Mitrev S (2012) Theoretical aspects of several successive two-step redox mechanisms in protein-film cyclic staircase voltammetry. *Electrochim Acta* 69:86–96
14. Mirceski V, Gulaboski R (2003) A theoretical and experimental study of two-step quasireversible surface reaction by square-wave voltammetry. *Croat Chem Acta* 76:37–48
15. Mirceski V, Gulaboski R, Lovric M, Bogeski I, Kappl R, Hoth M (2013) Square-wave voltammetry: a review on recent progress. *Electroanal* 25:24112422
16. Gulaboski R (2009) Surface ECE mechanism in protein-film voltammetry—a theoretical study under conditions of square-wave voltammetry. *J Solid State Electrochem* 13:1015–1024
17. Gulaboski R, Mihajlov L (2011) Catalytic mechanism in successive two-step protein-film voltammetry—theoretical study in square-wave voltammetry. *Biophys Chem* 155(1):1–9
18. Kokoskarova P, Maksimova V, Janeva M, Gulaboski R (2019) Protein-film voltammetry of two-step electrode enzymatic reactions coupled with an irreversible chemical reaction of a final product—a theoretical study in square-wave voltammetry. *Electroanal* 31: 1454–1464
19. Gulaboski R, Janeva M, Maksimova V (2019) New aspects of protein-film voltammetry of redox enzymes coupled to follow up reversible chemical reaction in square-wave voltammetry. *Electroanal* 31:946–956
20. Gulaboski R, Mirceski V, Lovric M (2019) Square-wave protein-film voltammetry: new insights in the enzymatic electrode processes coupled with chemical reactions. *J Solid State Electrochem* 23: 2493–2506
21. Mirceski V, Komorsky-Lovric S, Lovric M (2007) *Square-wave voltammetry, theory and application* (Scholz F, ed.) Springer, Berlin, Germany
22. Lovric M (2010) *Square-wave voltammetry in electroanalytical methods* (Scholz F, ed.) Springer, Berlin, Germany, 2nd edition
23. Mirceski V, Lovric M (1997) Split square-wave voltammograms of surface redox reactions. *Electroanal* 9:1283–1287
24. Gulaboski R (2019) Theoretical contribution towards understanding specific behaviour of “simple” protein-film reactions in square-wave voltammetry. *Electroanal* 31:545–553
25. Gulaboski R, Mirceski V (2015) New aspects of the electrochemical-catalytic (EC⁺) mechanism in square-wave voltammetry. *Electrochim Acta* 167:219–225
26. del Barrio M, Fourmond V (2019) Redox (in) activations of metalloenzymes: a protein film voltammetry approach. *ChemElectroChem* 6:4949–4962
27. Gulaboski R, Lovric M, Mirceski V, Bogeski I (2008) A new rapid and simple method to determine the kinetics of electrode reactions of biologically relevant compounds from the half-peak width of the square-wave voltammograms. *Biophys Chem* 138(3):130–137

Publisher's note Springer Nature remains neutral with regard to jurisdictional claims in published maps and institutional affiliations.